Photothermal Activatable Mucoadhesive Fiber Mats for On-Demand Delivery of Insulin via Buccal and Corneal Mucosa

Anna Voronova, Cristina Prieto, Maria Pardo-Figuerez, Jose Maria Lagaron, Amitav Sanyal, Bilal Demir, Thomas Hubert, Valérie Plaisance, Valérie Pawlowski, Séverine Vignoud-Despond, et al.

Photothermal activatable mucoadhesive fiber mats for on-demand delivery of insulin via buccal and corneal mucosa

Anna Voronova, [a] Cristina Prieto,[b] Maria Pardo-Figuerez, [b] Jose Maria Lagaron, [b] Amitav Sanyal,[c] Bilal Demir,[d] Thomas Hubert,[e] Valerie Plaisance, [a] Valerie Pawlowski,[a] Severine Vignoud,[e] Alexandre Barras, [a] Amar Abderrahmani,[a] Rabah Boukherroub [a] and Sabine Szunerits [a] *

[a] *Univ. Lille, CNRS, Centrale Lille, Univ. Polytechnique Hauts-de-France, UMR 8520-IEMN, F-59000 Lille, France*

[b] *Institute of Agrochemistry and Food Technology (IATA), Spanish Council for Scientific Research (CSIC), Calle Catedrático Agustín Escardino Benlloch 7, 46980 Paterna, Spain.*

[c] *Department of Chemistry, Bogazici University, Bebek, 34342, Istanbul, Turkey.*

[d] *CEA-TECH Region, Department Haut-de-France, 165 Avenue de Bretagne, 59000 Lille, France*

[e] *LETI-DTBS, CEA, 17 rue des Martyrs, 38054 Grenoble, France*

[e]*University Lille 2, CHU Lille, INSERM, European Genomic Institute of Diabetes (EGID), INSERM, UMR 1190, F-59000 Lille, France*

Abstract

Electrospun fiber mats loaded with therapeutics have gained considerable attention as a versatile tool in the biomedical field. While these bandages are largely based on fast-dissolving polymers to release the cargo, stimuli-responsive fiber mats have the advantages of providing a timely and spatially controlled drug delivery platforms, which can be refilled and reused several times. These qualities make electrospun fiber patches potential original platforms for painless and convenient on-demand hormone release. Because of the high need of more convenient and non-invasive method for delivering insulin, a hormone that currently treats hundred million people with diabetes worldwide, we have investigated the tremendous potential of reduced graphene oxide (rGO) loaded poly(acrylic acid) (PAA) based fiber mats as original

To whom correspondence should be send it: sabine.szunerits@univ-lille.fr

platform for buccal and corneal insulin delivery on-demand. The PAA@rGO hydrogel-like fibers rendered water-insoluble by incorporating β-cyclodextrin into the aqueous solution, followed by thermal crosslinking showed adequate tensile strength along with high adsorption capacity of insulin at pH 7 with good recyclability. The fiber mats maintain good fibrous morphology and high loading efficiency even after five loading–release cycles. The mucoadhesive nature of the fibers allowed their application for insulin delivery *via* the eye cornea and the buccal mouth lining, as evidenced in *ex vivo* studies. Insulin loaded PAA@rGO hydrogel-like fibers show an insulin flux via buccal lining of pigs of 16.6±2.9 μg cm^{-2} h^{-1} and J= 24.3±3.1 μg mL^{-1} h^{-1} for porcine cornea. Testing on healthy adult volunteers confirmed the excellent, mucoadhesive nature of the bandage, with three out of six 6 volunteers feeling completely comfortable (note 8.3) while wearing the patches in the buccal cavity.

Keywords: electrospinning, on-demand release, reduced graphene oxide, mucoadhesive

1. Introduction

Electrospinning of fiber mats incorporating therapeutic agents have become widely explored for the development of fast-dissolving drug delivery systems.[1-5] In contrast to other forms of drug carriers, such as liposomes and nanoparticles, electrospinning technology provides great flexibility in the therapeutic to be loaded into the fiber matrix and the material itself. [6] While electrospun drug reservoirs have high drug entrapment efficiency, the delivery of the drug is guided by drug diffusion out of the matrix, as well as by the degradation/dissolution of the carrier polymer. A different concept is the controlled release of active principles at a certain time point, putting the patient into the center of action. pH-sensitive electrospun fiber are one of the first-generation stimuli-responsive fiber mats. Polymers with acid-labile functional groups as acetal and hydrazone groups induce drug release at low pH.[7] While experimentally validated, the use of pH sensitive drug release from fiber mats for medical applications is currently limited to examples of treating inflamed issue.[8] On the other hand, temperature responsive fiber mats such as poly(N-isopropyl acrylamide) (PNIPAM), take advantage of the polymer's lower critical solution temperature (LCST) at 31-35°C, where at temperatures above LCST it becomes insoluble. While such polymers are efficient drug loading matrixes at low temperature due the increased porosity, they are less adapted for temperature-controlled drug release in the form of external bandages on the human body. Electrospun fiber mats where an increase in temperature results in swelling of its 3D scaffold and drug release are more adapted for such applications. Some of us have demonstrated lately the utilization of reduced graphene oxide (rGO) loaded poly(acrylic acid) (PAA) based hydrophilic nanofiber matrix for photothermal release of antibiotics. PAA was electrospun in the presence of beta-cyclodextrin (20 wt.% of PAA) as a cross-linker. The formed PAA@rGO matrix features good photothermal heating properties reaching 51±2 °C upon laser (980 nm) irradiation at a power density of 1 Wcm^{-1}.

The specific features of electrospun polymer fiber mats such as high surface-volume ratio and interconnected nonwoven architecture provides them with mucoadhesive properties and should be considered for transmucosal drug carrier systems. [9] In addition, transport of molecules across the buccal membrane is far simpler than the skin, alveoli or intestinal membranes. Therefore, mucoadhesive drug delivery is expected to improve drug bioavailability, to increase the patients' s therapy compliance, to sustain drug delivery and a relatively rapid onset of action with the possibility to remove the formulation if therapy is required to be discontinued.[10-11] Through less permeable that the sublingual area, the buccal oral cavity provides an ideal

targeting zone. The buccal mucosa is well-vascularized, allowing drugs to be rapidly absorbed into the venous system underneath the oral mucosa. Being different from transdermal drug delivery route, mucosal surfaces are lacking the stratum corneum barrier, resulting in faster drug delivery. The inherent barriers for efficient buccal mucosal drug delivery are the keratinized tissue and the elimination of the drugs to the flashing action of saliva in the absence of uni-directional mucoadhesive mouth patches.[12]

We investigate, in this study, the usefulness of the PAA@rGO matrix as mucoadhesive films for buccal linings and insulin release (**Figure 1**). We speculated that the presence of ionizable groups such as carboxyl groups of PAA and rGO together with hydroxyl groups of the cyclodextrin cross-linker ensures the interaction with the mucosal membranes. Indeed, results of mucoadhesive studies confirmed excellent muco-adhesion. *In vitro* insulin release studies and *ex vivo* permeation studies using pig cheek lining and cow eyes demonstrated the possibility to deliver insulin *via* mucosal membranes and might open new ways for insulin therapy, which is so far based on multiple daily subcutaneous needle injections through pen or catheters connected to pumps. These methods are both painful and inconvenient, and significantly deteriorate the life quality of patients and lead patients to neglect or even give up the therapy.

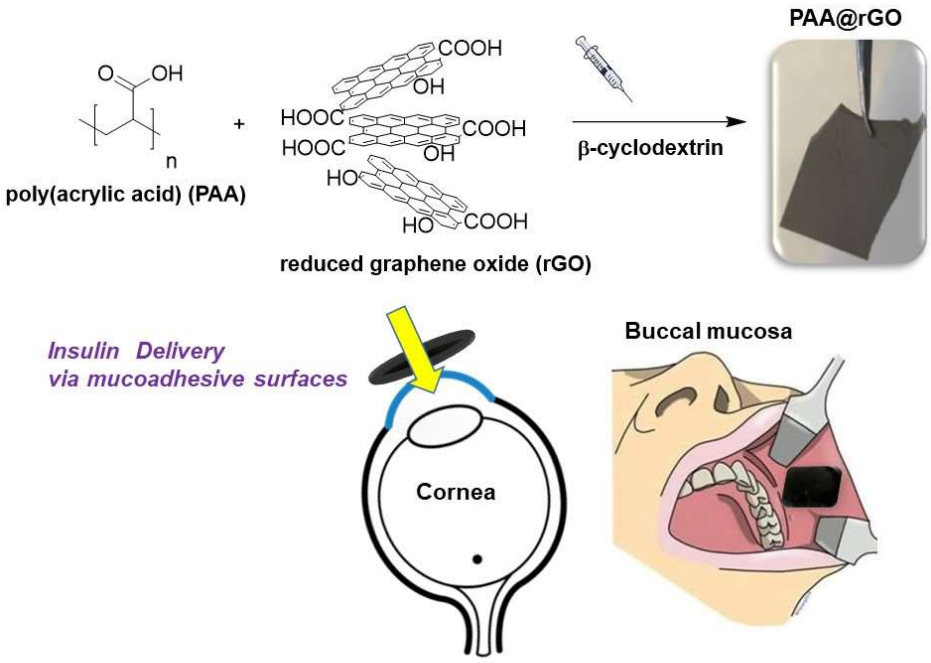

Figure 1. Illustration of the formation of β-cyclodextrin cross-linked PAA@rGO nanofiber mats using electrospinning method and its use for on-demand insulin release *via* mucoadhesive

interfaces such as cornea and buccal mucosa. *Ex vivo* examples: cow cornea and pig buccal lining.

2. Results and Discussion

2.1. Characteristics of mucoadhesive PAA@rGO fiber mats

Mucoadhesive patches were fabricated by electrospinning a mixture of PAA, β-cyclodextrin (20 wt.% of PAA) and rGO (2.4 wt.%). The bandages consist of a dense fiber mat (**Figure 2a**) with fibers of 400±150 nm in diameter. Most importantly, PAA@rGO were water-insoluble and the fibrous nanostructures remained preserved even upon immersion for 1 week in water at 37°C (**Figure 2b**). This contrasts with rGO-free PAA fibers which dissolve immediate after immersion in water. The PAA@rGO films proved to be also stable upon immersion into saliva (**Figure 2c**). This makes it different to others works for which the nanofiber film disintegration was initiated upon contact with stimulated salivary fluid in a time frame of about 150 s.[13]

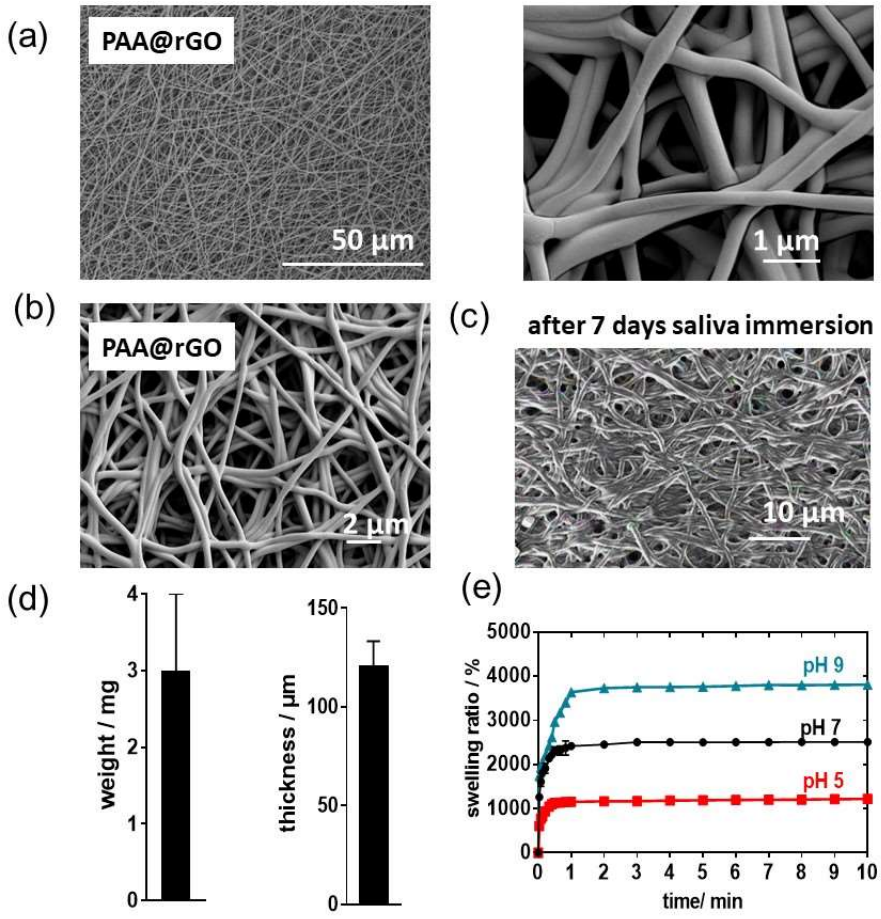

Figure 2. Characteristics of mucoadhesive PAA@rGO fiber mats: (**a**) SEM images at different magnifications. (**b**) SEM of PAA@rGO after immersion for 1 week at 37°C in water.

(**c**) Stability of the nanofiber film in salivary fluids. (**d**) Weight and thickness characteristics of four different batches of PAA@rGO. (**e**) Swelling behavior in water over time as a function of pH.

Fiber mats assessed from four different batch fabrications were observe to have an average weight of 3.2±1.0 and thickness of 120±18 µm (**Figure 2d**). The degree of swelling was fast **(Figure 2e**), reaching up to 2000 % of its weight in the first 30 s and a steady state after 1-2 min. Swelling was stronger in alkaline pH. The results of swelling behavior correlate with other works,[5] where the swelling ratio increased with increasing solution pH.

The presence of rGO was validated by the characteristic Raman bands at 1350 cm^{-1} (D-band) and 1580 cm^{-1} (G-band) (**Figure 3a**). The presence of rGO endows the mucoadhesive patch with photothermal properties (**Figure 3b**). Irradiation of PAA@rGO with a near infrared laser (980 nm, 500 $mWcm^{-2}$) resulted in a surface temperature of 51±2 °C within 5 min. The mechanical properties of PAA@rGO were assessed in addition (**Figure 3c**). The maximal displacement at which the applied force dropped abruptly is identified as the breaking point[14] between the patch and the mucoadhesive surface, buccal tissue in our case. PAA@rGO adheres well to the buccal tissue and shows a mucoadhesive force of 0.74±0.3 N cm^{-2}, in the order of reported mucoadhesive forces.[15]

The biocompatibililty of PAA@rGO mats was assessed on the HeLa and ARPE-19 cell lines (**Figure 3d)**. The toxicity was evaluated using the resazurin assay, based on the conversion of non-fluorescent dye to a fluorescent molecule by mitochondrial and cytosolic enzymes. No loss in cell viability and loss of metabolic activities was observed upon incubation of both cells for 24 h respectively. Lack of cytotoxicity suggests that no residual monomers, which could lead to potential cytotoxicity, are. Furthermore, eventual detrimental effect of thermal activation of PAA@rGO gel on cell viability was determined. Thermal activation of the of PAA@rGO mats for 10 min at 500 mW cm^{-2} did not induce any change in cell viability.

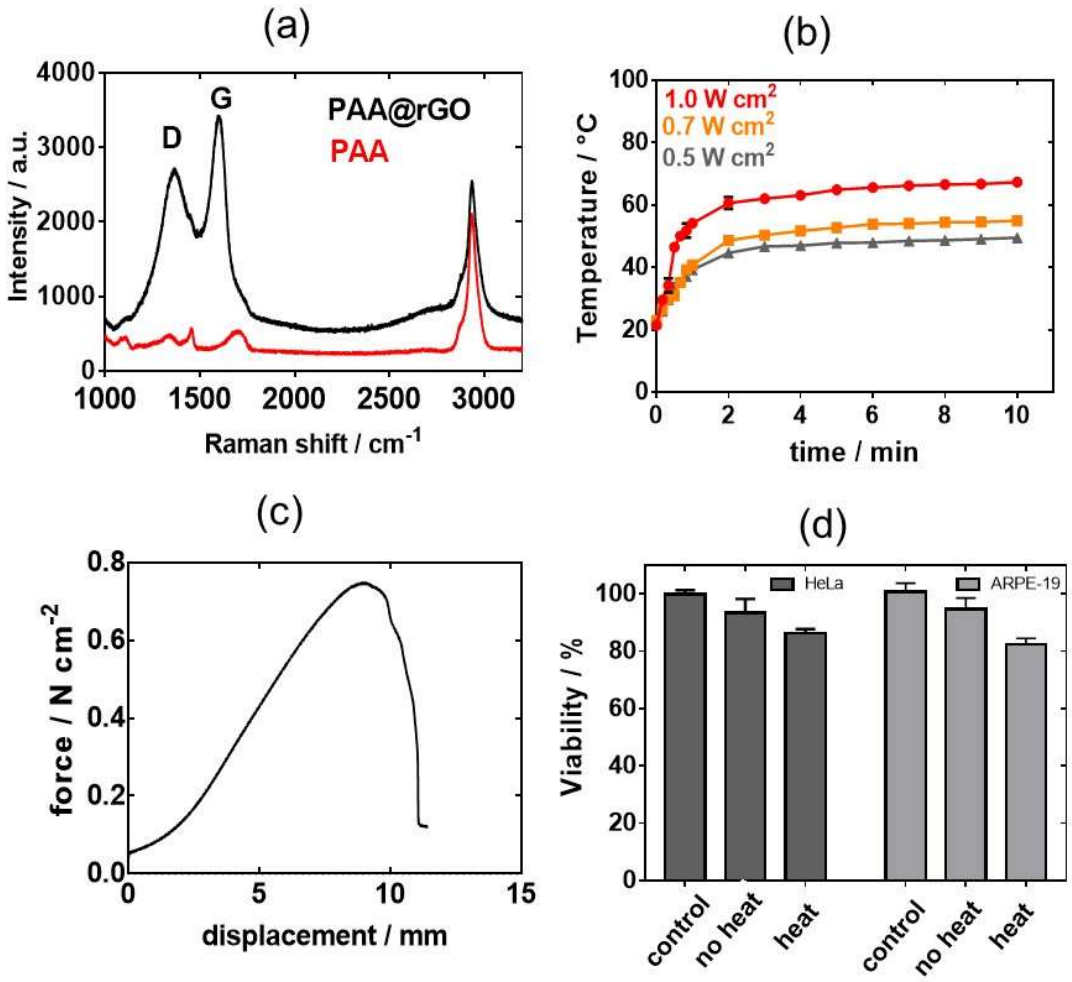

Figure 3. Characterization of PAA@rGO: (**a**) Raman spectra of PAA and PAA@rGO mats. (**b**) Photothermal heating curves of the patch at 980 nm illumination as a function of power density (0.5-1 W cm^{-2}). (**c**) Tensile tests via Force-displacement curve of PAA@rGO on porcine buccal mucosa. (**d**) Cell viability of ARPE-19 and HeLa cell in the presence of PAA@rGO without and with heat activation at 0.5 W cm^{-2} for 10 min.

2.2. Insulin-loaded mucoadhesive PAA@rGO patches

We opted for using insulin as a model drug given that diabetes is one of the leading causes of early mortality worldwide.[16] As all current antidiabetics are unable to achieve a long-term glycemic control, insulin administration remains currently the only option to control blood glucose levels efficiently. To decrease blood glucose concentrations, 250-330 nM (145-192- µg mL^{-1}) of insulin is needed. Human insulin (200 µg mL^{-1}) was consequently integrated into PAA@rGO fiber mats through their simple immersion for 3 h under continuous shaking at 4 °C. The loading capacity for human insulin was evaluated through the determination of the concentration of insulin in solution before and after loading using HPLC, as reported by us

recently.[17] Insulin could be efficiently loaded (89% loading efficiency) onto the mucoadhesive patches over a time span of 60 min (**Figure 4a**). These loading efficiencies are comparable to rGO loaded hydrogels (80%), as reported by some of us.[18] The loading capacity was found to be pH-dependent, with a higher insulin loading at pH 4 (**Figure 4a**). At pH 5, insulin is positively charged and interacts more strongly with the negatively charged backbones of PAA@rGO fibers.

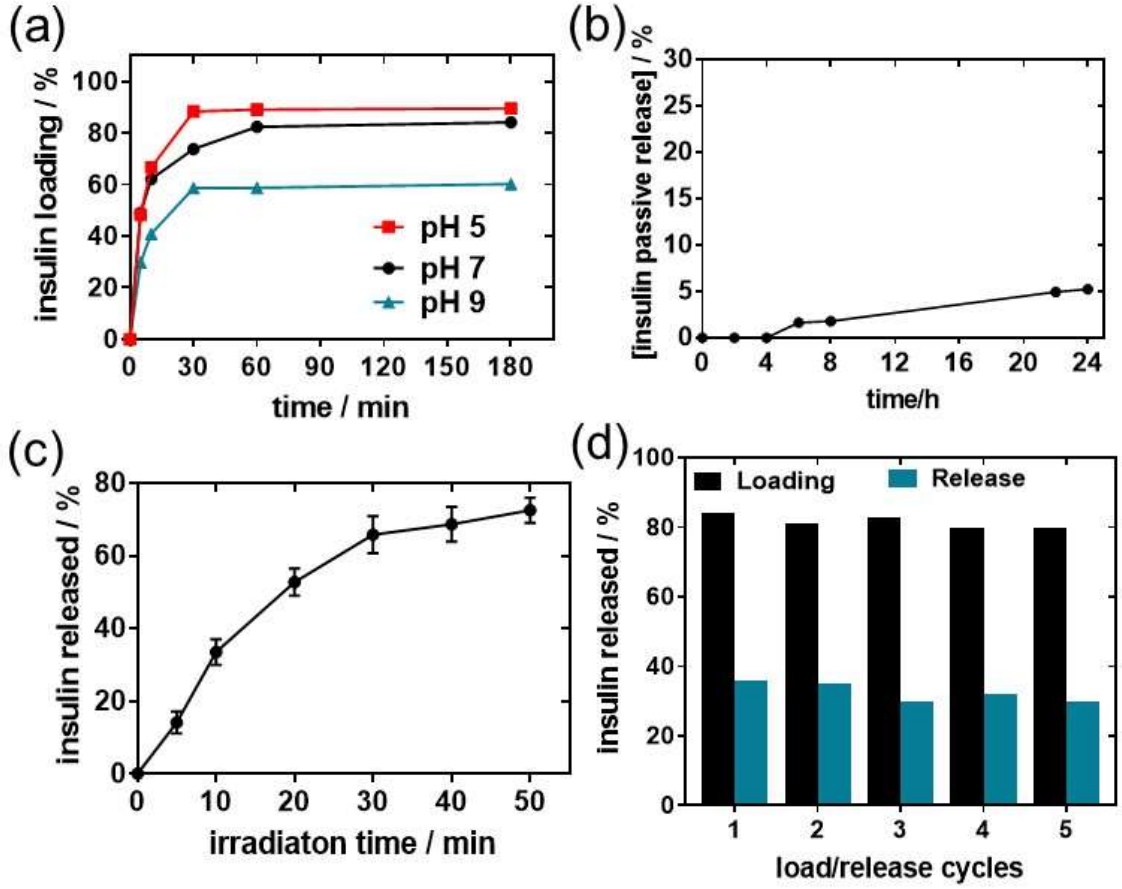

Figure 4. Insulin loaded PAA@rGO. (**a**) Human insulin (200 µg mL^{-1}) loading capacity as a function of solution pH. (**b**) Passive release over time. (**c**) Photothermal release with time upon illumination at 980 nm using a laser power of 0.7 W cm^{-2}. (**d**) Loading and release of insulin into the bandage.

To determine the amount of insulin passively released from the mucoadhesive patch, the patch was immersed for 24 h in a solution of pH 7.4 (**Figure 4b**). About 5% of insulin was released, mostly due to some insulin being present outside the patch while most remained entrapped. Most important, after 24 h, no further insulin was released. This contrasts with the amount of insulin released upon photothermal irradiation for 10 min (**Figure 4c**). The good heating

capacity of the mucoadhesive patch results in an efficient heat triggered insulin release, reaching 150 µg (75%). Besides the sufficient photothermal release, PAA@rGO fiber mats featured appropriate reusability. Reloading of the mats with insulin followed by photothermal activation for 10 min could be performed with the same efficacy for 5 successive cycles.

2.3 *Ex-vivo* insulin permeation analysis

The distinct keratinization of the oral mucosa negatively impacts on the passage of drugs through the mucosa and limits therapeutic efficiency.[19] The absorption of insulin from the patches through buccal mucosa (**Figure 5a**) has been assessed in the following by *ex vivo* permeability studies, using pig-based models with close resemblance to the human buccal mucosa.[15, 20] For this, porcine buccal mucosa was separated from the underlining tissue using a scalpel and rinsed with PBS and fitted into Franz diffusion cells within 2 h after harvesting to preserve the membrane permeability and to ensure tissue integrity. To determine the permeability of insulin, electrospun fiber mats patch (1.5×1.5 cm^2, 2 mg) was loaded with 500 µg mL^{-1} of insulin by immersion into 1 mL solution at 4 °C for 1 h. With a loading efficiency of 82% (**Figure 4a**), this accounts for 410 µg mL^{-1} insulin integrated to the patch. This patch was placed on the top of the porcine buccal mucosa (**Figure 5b)** and both passive and heat-initiated permeations of insulin were assessed (**Figure 5c**). As expected, without heat activation, the insulin-loaded fiber mat showed limited insulin permeation through the epithelial cells of the porcine mucosa. In contrast, photothermal laser activation for 10 min resulted in substantial insulin penetration across the buccal tissue. After 6 h, 12±2% of insulin (which accounts for 41.1 µg mL^{-1} insulin) has permeated the porcine mucosa model, with about 16±1 % of insulin having been detected in the porcine lining. In total, the heat activated patches were able to transport 28±2 % (82 µg mL^{-1}) of the loaded insulin into the buccal lining. These findings are in line with recently reported buccal patches by Vaidya and Mitragotri using insulin loaded biodegradable polymeric patches using chitosan as mucoadhesive matrix and ionic liquids (ILs)/deep eutectic solvent (DES) as the transport facilitator.[15] An insulin flux of 16.6±2.9 µg cm^{-2} h^{-1} was recorded, being considerably elevated compared to that previously reported for photothermal activated insulin flux *via* porcine skin (as J=0.8±0.2 µg cm^{-2} h^{-1}).[18] It is in comparable with results by some of us using an electrothermal activation approach with a flux of 15.6 ± 1.3 µg cm^{-2} h^{-1} [17]and in line with insulin delivered from poloxamer-407 gels using transdermal iontophoresis in the presence of menthone as a skin enhancer.[21] As the buccal mucosa is deficient of a stratum corneum layer, insulin can pass unhindered into the entire

buccal epithelium. The efficient mucosal insulin delivery under heat might further arises from the fluidization of the upper epithelium of the buccal tissue upon temperature increase, thereby indicating a paracellular mode of insulin transport. Fluorescence analysis of harvested buccal tissue before and after heat treatment and delivery of FITC-label insulin (**Figure 5d**) showed no structural damage of the tissue at the application site with the fluorescence signal remaining localized to the outside the tissue without heat application. After 10 min heat application and observing the fluorescence stained tissue after 6h, fluorescence of 500 µm in depth is observed, equal to the thickness of buccal nonkeratinized structures. Eventual, the increased temperature induces mucus thinning effect and the protective role of PAA@GO against saliva proteases could be reasons for the efficient insulin delivery.

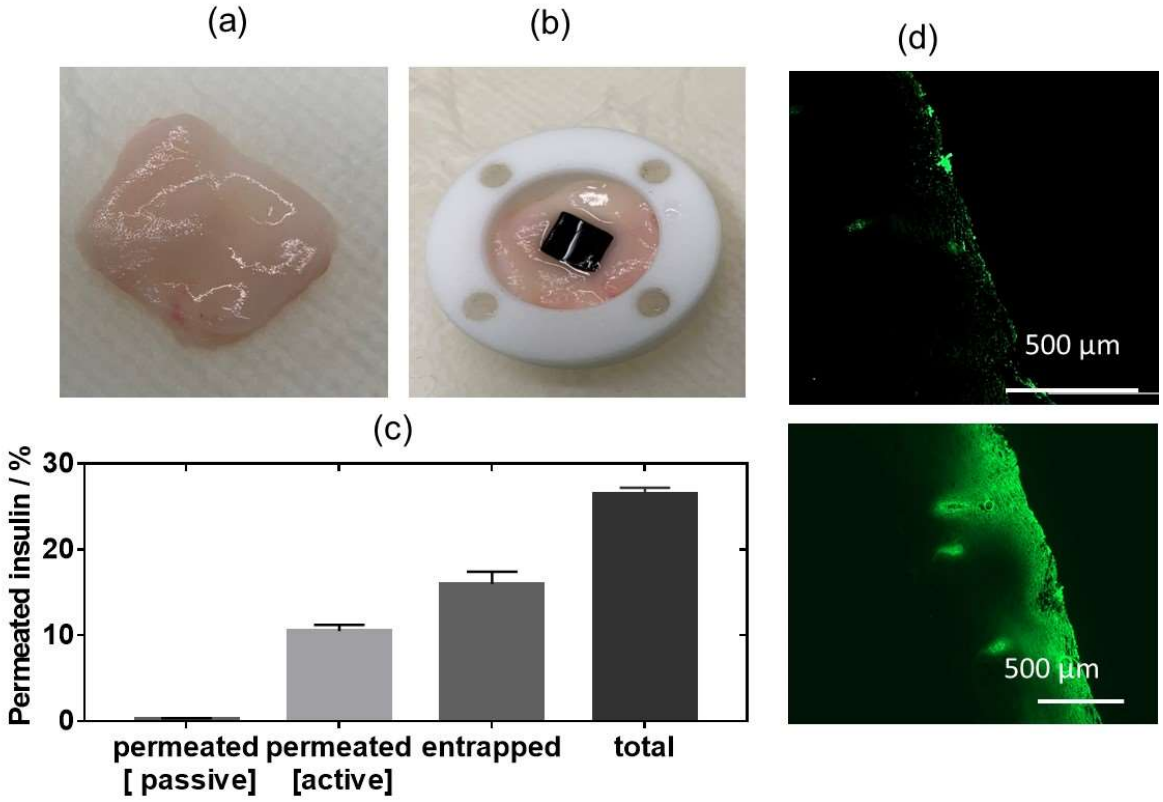

Figure 5. *Ex-vivo* insulin permeation studies of insulin-loaded PAA@rGO nanofiber mats *via* porcine buccal mucosa: (**a**) Photographic image of porcine buccal tissue harvested and used for permeation studies. (**b**) Photograph of porcine buccal tissue fixed into Franzen diffusion cell and immobilization of insulin-patch on top. (**c**) Cumulative permeation profile of insulin through the buccal tissue after 6 h upon passive or photothermal activation (10 min action with laser at 980 nm) (n=3). Error bars represent means of ± SEM. (**d**) Fluorescence images of buccal tissue treated with a FTIC-insulin loaded PAA@rGO patch with (left) and with (10 min, 980 nm, 500 mW cm^{-2}) activation.

In addition, comparable experiments were performed on pig cornea (**Figures 6a, b**), coated with a mixture of mucus, epithelial cells, proteinaceous and lipoidal material that adhere firmly to the corneal surface. Permeation of insulin via the pig cornea was comparable to that of pig buccal mucosa, with limited passive diffusion; 13±1% of insulin permeated the cornea and 25±1% remained on the cornea tissue after 6 h, corresponding to a total insulin of 37±1% i.e. 151± 3 μg mL^{-1} and an insulin flux of 24.3±3.1 μg mL^{-1} h^{-1} (**Figure 6b**). This flux is several-times larger than that achieved using photothermal activation via porcine skin and 1.5 times using buccal mucosa.

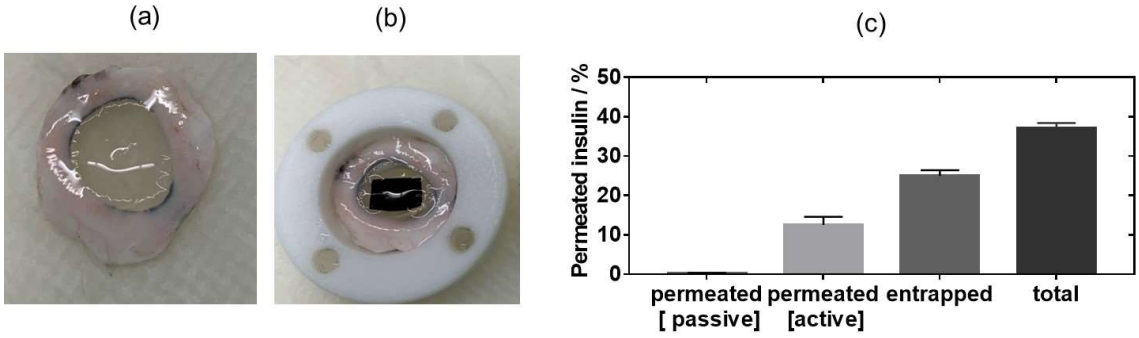

Figure 6. *Ex-vivo* insulin permeation studies of insulin-loaded PAA@rGO nanofibers mats *via* porcine cornea: (**a**) Photographic image of porcine buccal tissue harvested and used for permeation studies. (**b**) Photograph of porcine buccal tissue fixed onto Franzen diffusion cell and immobilization of insulin-patch on top. (**c**) Cumulative permeation profile of insulin through the buccal tissue after 24 h upon passive or photothermal activation (10 min irradiation at 980 nm, 500 mW cm^{-2}) (n=3). Error bars represent means of ± SEM.

2.4 *In-vivo* mucoadhesive properties and acceptability of PAA@rGO nanofibers mats by volunteers

Pancreatectomized Gottingen minipigs are valuable models of insulin-dependent diabetes as they share many similarities with humans such as the morphology of the pancreas and the overall metabolic status of the two species. To investigate the efficiency of the nanofiber mat to lowering blood glucose level (BGL), insulin (100 μg mL-1 corresponding to 2.88 Insulin units) was loaded into the PAA@rGO fibers and applied inside the buccal cavity of the pig (**Figure 7a**). After thermal activation of the fiber mats for 10 min an immediate reduction of the BGL was observed (**Figure 7b**). In the control experiment without thermal activation, the BGL remained constant over the same time period. The decrease of the BGL agrees with an increase in the plasma insulin concentration, confirming the hypoglycemic effect of insulin

released from the patch (**Figure 7c**). It furthermore coincides with the insulin plasma profile of subcutaneous injected insulin (2.88 IU). **Figure 7d** shows furthermore the buccal lining after removal of the insulin-loaded PAA@rGO fiber mat indicating no irritation and visual degradation of the mucus lining;

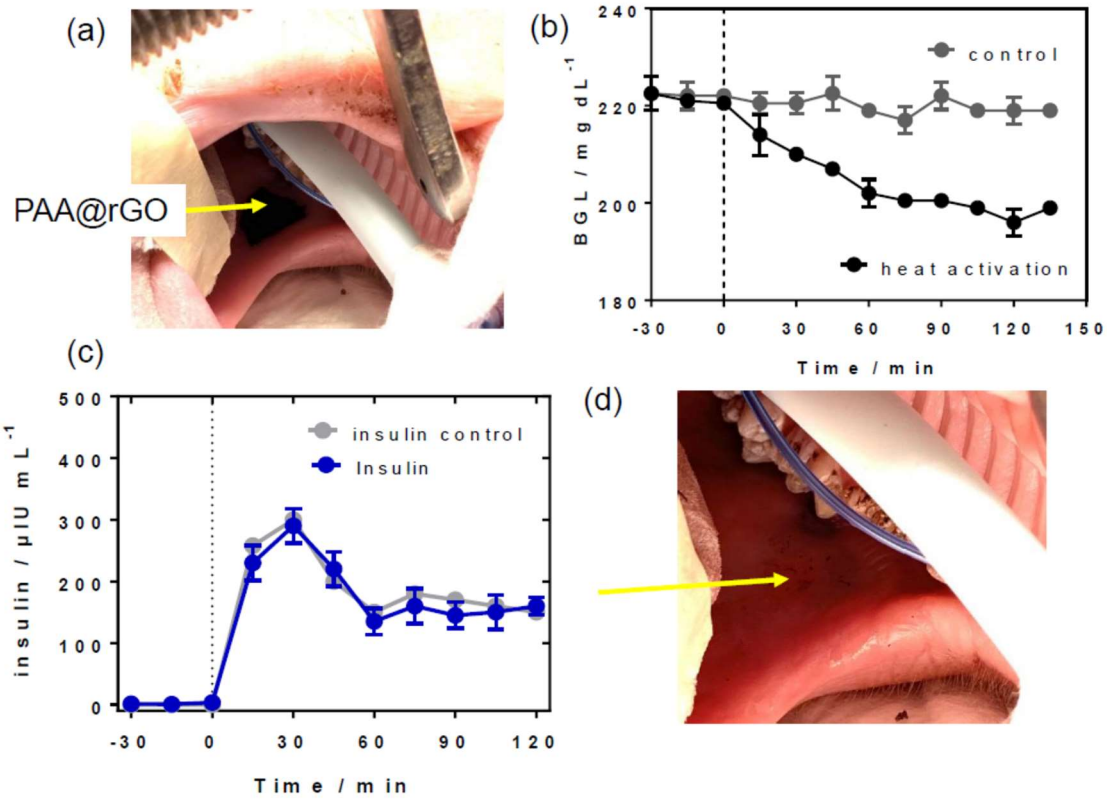

Figure 7. *In Vivo* Permeation Study of insulin from PAA@rGO fiber mats via the buccal lines of mini-Pigs: (a) Image of pig buccal cavity in the presence of the PAA@rGO fiber mat. (b) Effect of insulin (2.88 IU) loaded PAA@rGO fibers mats on blood glucose level (BGL) over time after 10 min thermal activation (black) and with no heat activation (grey). (c) Time dependent blood insulin level in minipig. In a control experiment (bright blue), insulin was injected subcutaneously (2.88 IU) and blood insulin was dosed over time. (d) Image of buccal cavity after PAA@rGO fiber mat removal.

2.5. *In-vivo* mucoadhesive properties and acceptability of PAA@rGO nanofiber mats

Finally, we applied PAA@rGO nanofibers mats to 6 healthy adult volunteers (3 male, 3 female) aged between 25 and 49 years to obtain information about *in vivo* residence time and patch acceptability (**Figure 8a**).The adhesion evaluated for a time span of 120 min was excellent, with all bandages residing for 120 min in the 6 cases f (**Figure 8b**). The volunteers rated the

patch as excellent (note of 9.3) with most of volunteers feeling comfortable (note 8.3) while wearing the patches in the buccal cavity. 2 male volunteers considered it "mentally" difficult to have a nanomaterial in the mouth and the discomfort was related to this rather than the bandage itself. All volunteers agreed that the patches have no taste (note 10). The rating for removing the bandage is evaluated as medium (note of 6.1) indicating that it remains difficult to remove the bandage once installed removal easy. None of them reported interference with speak nor effects on saliva production and swallowing.

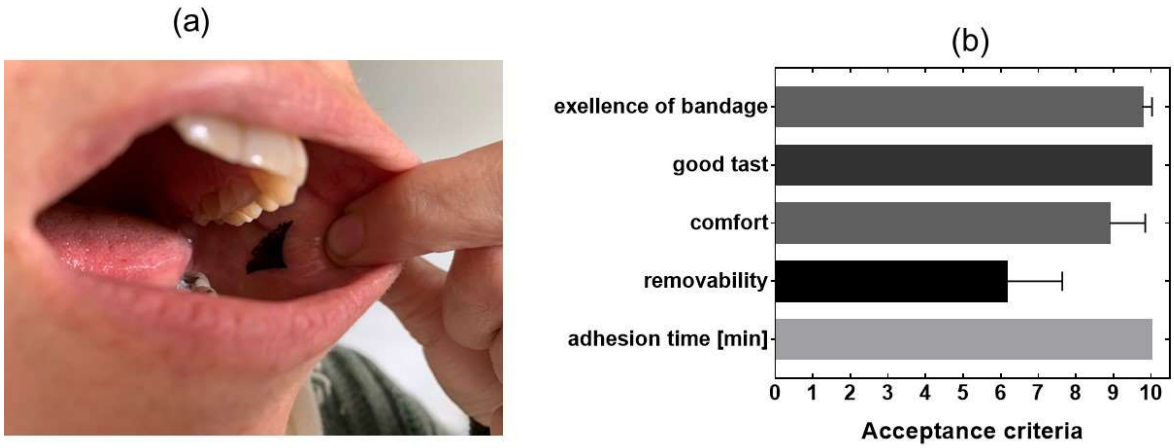

Figure 8. *In-vivo* mucoadhesive performance of PAA@rGO nanofibers mats placebo: (**a**) Photograph of placement of mucoadhesive patches in humans attached by 5 s pressure application. (b) Acceptability evaluation of 6 adult volunteers on the adhesion time, overall bandage excellent, comfort, taste and removability in a scale of 0 (bad)- 5 medium-10 (excellent)

3. Conclusion

In summary, we have demonstrated that incorporation of reduced graphene oxide (rGO) into a water insoluble fiber mats, formed from poly(acrylic acid) (PAA) and β-cyclodextrin cross-linker by electrospinning, leads to the formation of water insoluble hydrogel with good photothermal characteristics. The resulting hydrogel fiber mat allowed efficient loading of a therapeutic peptide like insulin, while maintaining its good fibrous morphology. Using porcine buccal mucosa as well as porcine cornea as *ex vivo* models, the flux of insulin across the mucosal lining recorded upon passive or photothermal activation was investigated. As in the case of previously reported photothermal transdermal insulin delivery, thermal activation resulted in strongly increased insulin permeation rates reaching J=16.6±2.9 μg cm^{-2} h^{-1} for

buccal mucosa and J= 24.3±3.1 μg mL^{-1} h^{-1} for porcine cornea, being several times more elevated to comparable transdermal delivery. This result confirms that buccal mucosa is suitable for the non-invasive delivery of insulin via electrospun fiber mats-based mucoadhesive patches. Efficient release of insulin by photothermal activation supports the idea of using mucoadhesive patches containing insulin for treating patients with diabetes. In type 2 diabetes, the most prominent form of diabetes, basal insulin therapy is often added to oral diabetes medication regimens that do not provide optimal glucose management. In general; this biotherapy does not require high dose of insulin. The quantity of insulin released from our mucoadhesive patches could be in line with their use in basal therapy. Therefore, compared to multiple insulin injection, this mode of delivery offers a huge advantage by increasing the compliance of patients to treatment, as it is resilient and can be easily self-administrated. In this perspective, our study allows future preclinical studies aiming to test the efficiency of this original platform to on-demand deliver insulin and to treat diabetes in animal models of diabetes. Although these dates cannot be directly related to human buccal mucosa since porcine mucosa epithelium is about 3-times thicker than in humans, insulin released from PAA@rGO fiber mats clearly show to penetrate buccal mucosa lining deeply.

4. EXPERIMENTAL SECTION

4.1. Materials

Polyacrylic acid (PAA, Mn 450 000 g mol^{-1}), β-cyclodextrin, recombinant insulin, insulin FITC, artificial saliva, phosphate-buffered saline (PBS, pH 7.4), sodium hydroxide and hydrochloric acid were purchased from Sigma-Aldrich. Reduced graphene oxide (rGO) in powder form was purchased from Graphenea (Spain).

4.2. Electrospinning of nanofiber mats

The electrospinning of nanofiber mats was performed according to the procedure described by us previsouly.[22] Briefly, dispersed aqueous rGO solution (1 mg mL^{-1}, 2.4 wt.%) was mixed with PAA (81.4 wt.%), and β-cyclodextrin (16.2 wt.%) and kept under magnetic stirring overnight. The resulting clear solution was electrospun using a 1 mL syringe fitted with a 14-gauge blunt needle at the rate of 0.35 mL min^{-1} at 15 kV. The distance was kept at 15 cm during the electrospinning process. Resulting electrospun fibers were cross-linked under vacuum at 140 °C for 30 min.

4.3. Determination of swelling degree

The swelling degree of PAA@rGO nanofibers was determined following the method reported by Mittal et al. The nanofiber mat was cut into smaller pieces (1×1 cm) and dried at 70 °C for 24 h before weighting. The dried samples were then immersed in Milli-Q water at room temperature for 1 h and taken off at given time intervals (2s-10 min). The nanofiber pieces were dried with a cotton tissue in order to remove any remaining water and weighted using a microbalance. The swelling ratio of nanofiber mats was calculated as following:

$$\text{Swelling degree (\%)} = \frac{Wt-}{Wd} \times 100$$

where W_t is the weight of wet nanofibers at time t and W_d is the weight of dry nanofibers.

4.4. Determination of weight, thickness and pH of nanofiber mats

The measurements of weight, thickness and pH were performed in triplicates on randomly selected patches from independent batches. The thickness was determined using a thickness gage ID-C112XBS from Mitutoyo Corporation (Japan). For weight determination, the mats of 1×1cm^2 in size were weighted on a digital balance. The pH value was recorded using a pH meter (Hanna Instruments, Rhode Island, US) by immersion of the nanofiber mats into water for 2 min.

4.5. Drug loading

Insulin-FITC and insulin loaded patches were produced by immersion of 3.0±1.0 mg PAA@rGO electrospun mats into 1 mL (200 µg mL^{-1}) of insulin-FITC or insulin aqueous solutions under continuous shaking at 150 rpm for 4 h at 4°C.

4.6. *In vitro* photothermal drug release studies

In vitro drug release experiments were performed in 1 mL 1× PBS solution (pH 7.4). The nanofiber mats were irradiated with a continuous mode laser (Gbox model, Fournier Medical Solution) with an output light at 980 nm at power densities 0.5, 0.7 and 1 W cm^{-2} for 10 min. The temperature change was captured by an Infrared Camera (Thermovision A40) and treated using ThermaCam Researcher Pro 2.9 software. The amounts of insulin and rhodamine B

released were evaluated by high-performance liquid chromatography (HPLC) of the solution collected after irradiation using calibration curves generated for each drug.

4.7. Cytotoxicity tests of PAA@rGO bandage

The ARPE-19 spontaneously immortalized cell line of human retinal pigment epithelium and the e HeLa cells, derived from cervical carcinoma from a 31-year old female [ATCC® CCL-2™, ECACC, Sigma Aldrich, Saint-Quentin Fallavier, France], were cultured and maintained in Dulbecco's Modified Eagle's medium (DMEM, Gibco®) high glucose with 2 mM Glutamine, DMEM/F12 media with 2 mM Glutamine and DMEM supplemented with 10% fetal bovine serum (FBS, Gibco®) and 1% penicillin-streptomycin (Gibco®), respectively, in a humidified incubator at 37 °C and 5% CO_2. Cells were seeded at a density of 10^4 cells/well in a 96-well plate and grown for 24 h before assay.

The cell viability of PAA@rGO was evaluated using resazurin cell viability method. Briefly, 1 mL of the resazurin solution (11 µg mL^{-1}) in complete medium was added to each well containing the gel and the plate was incubated for 4 h in the humidified incubator. The fluorescence emission of each well was measured at 593 nm (20-nm bandwidth) with an excitation at 554 nm (18-nm bandwidth) using a Cytation™ 5 Cell Imaging Multi-Mode Reader (BioTek Instruments SAS, France). Each condition was replicated three times

4.8. *Ex-vivo* permeation experiments

All animal studies were conducted at the Plateforme de Recherche Expérimentale (University of Lille, France) in accordance with the ethnic protocol entitled "Délivrance transdermique, de substances pharmacologiques, contrôlée par l'utilisation d'une énergie thermique chez la souris et le mini-porc" (Nr APAFIS#21080-2019111511521244). 3 female mini-pigs weighting 10-16 kg were used . *Ex-vivo* permeation experiments were performed using cornea and buccal mucosal lining from pigs. Fresh porcine buccal mucosa was separated from the underlining tissue using a scalpel and stored in PBS 1× at 4 °C not more than 12 h before the permeation experiment. Tissue with any visual damage was discarded. Intact mucosa was immersed in deionized water at 65 °C for 60 s in order to separate the epithelium from the connective tissue as reported previsouly.[23] Mucosa samples (thickness 310±80 µm) were gently cut into pieces (1cm^2) and placed between the chambers of Franz diffusion cell and *ex-vivo* experiment was performed. In the case of pig cornea, they were gently cut into 1.8 cm^2 circular pieces prior to their use in the Franz diffusion cell.

Insulin skin diffusion experiments were carried out using static Franz diffusion cells (Proviskin, France), exhibiting an effective area of 0.785 cm^2. The receptor chamber was filled with 1× PBS (pH 7.4) solution and maintained at 37 °C using a circulating bath (Julabo) with magnetic stirring at around 500 rpm. The cornea pieces were carefully clamped between the donor and the receptor chambers (8 mL) and pre-incubated for 20 min. The drug loaded electrospun mats were irradiated with a continuous wave laser at 980 nm for 10 min (laser power=1 Wcm^{-2}). At determined time intervals, 300 µL aliquots of diffused solution were removed from the receptor compartment and analyzed by HPLC. After each sampling, an equal volume of fresh diffusion medium was added to the receptor chamber.

Evaluation of insulin trapped in the *ex vivo* sample was performed by adding the species into water/ice mixture for 10 min and sonicated in the presence of ZnO_2 beads (4 mm in diameter), before being centrifuged for 30 min at 13500 rpm using an ultracentrifuge (Mini Scan Fuge ORIGIO). The liquid phase was collected and filtrated through a 0.1 µm Nylon filter (Whatman Puradisc 13 mm) and the amount of insulin was determined by HPLC/UV.

4.9. In-vivo experiments using Mini-Pigs

Insulin delivery in vivo was tested on female domestic pigs (three) weighing 50-62 kg. The animals were subjected to total pancreatectomy a day before each experiment. A tunneled central venous catheter into the external jugular vein was placed in each animal facilitating a blood sampling. The insulin loaded patches (2.8 IU) were placed inside the buccal lining of the pig moth. No fixing is needed due to the excellent mucoadhesive character of the patch. The PDD@rGO patch was activated for 10 min giving the temperature ~50 °C. Glucose levels were measured directly from fresh blood via central catheter using a commercial glucometer. Blood samples were obtained at and different time intervals. Blood samples were centrifuged at 5.000 rpm for 10 min at 4 °C and plasma was immediately separated and stored at –80 ° C until analyzed. Radioimmunoassay kits were used for the measurements of insulin (Bi-Insulin RIA ® ; Bio-Rad, Elexience, Verrières-le-Buisson, France). All the manipulations in pigs, including total pancreatectomy, placing of the catheter, microneedles and patch activation as well as blood samplings, were performed under general anesthesia with a 2-3% concentration of isoflurane (Aerrane; Baxter, France) and under analgesia with transcutaneous fentanyl (Recuvyra ; Elanco; France). Animal studies were approved by the Institutional Ethics Committees for the Care and Use of Experimental Animals of the University of Lille (protocol n°21080). All experiments were performed in accordance with the guidelines for animal use specified by the European Union Council Directive of September 22, 2010 (2010/63/EU).

4.10. *In-vivo* residence times

The residence time was evaluated on 6 volunteers (3 male and 3 females). Following the international standard of Good Clinical Practices, placebo patches (15×12 mm) were applied to the buccal mucosa for 5 s with applied pressure. Patch adhesion was monitored for 2h and residence time determined. The residence time was considered as the time until the patch dropped from the buccal mucosa. An acceptable questioner was completed by each volunteer to obtain information about parameters such as taste, comfort, dry mouth and salivation.

4.10. Data analysis

Results are presented as mean± standard deviations unless overwise stated. Statistical analysis all date was carried out using GraphPad prism version 7.0 (GraphPad software Inc., San Diego, USA). All experiments were conducted at least in triplicate.

4.11. Characterization

Fourier transform infrared spectroscopy (FT-IR) analyses were performed on Thermo Fisher Scientific Inc, Nicolet 380. **Raman spectroscopy measurements** were recorded on a LabRam HR Micro-Raman system (Horiba Jobin Yvon, France) using a 473-nm laser diode as excitation source. **Scanning electron microscopy (SEM)** micrographs of prepared mats were performed with an electron microscope Hitachi S-4800 FE-SEM (Hitachi Technologies Corp., Tokyo, Japan). The samples were sputtered with a gold/palladium layer before scanning. The accelerating voltage was 10 kV, the probe current was 9800 nA. **Mechanical properties** of elastomeric PAA-@rGO fibers were investigated via a TAXT plus C Texture Analyzer. The fiber samples were soaked in water and squeezed between tensile grips; a tension test was applied using the following parameters with a pre-test speed of 1.0 mm/s, test speed of 0.5 mm/s and a post-test speed of 10 mm/s. Tensile test was performed until seeing a macroscopic damage of the fibers. Relative analysis was applied to calculate stress, strain and Young modulus of elasticity. **The photothermal effect** of the fibers was assessed using a 980 nm-continuous wave laser (Gbox model, Fournier Medical Solution) with an output light at 980 nm at power densities 0.5, 0.7 and 1 W cm^{-2} . This laser was injected into a 400 μm-core fiber and placed at 6 cm from the bottom of the wells. The output was not collimated and the resulting beam divergence allowed to illuminate uniformly up to 4 wells. The temperature changes on the surface of the nanofiber mats were captured by an infrared camera (Thermovision A40) and treated using

ThermaCam Researcher Pro 2.9 software. **The tissue cuts** were done using The Leica CM3050 S cryostat (thickness of 10 µm) and visualized with Cytation™ 5 Imaging multi-mode reader

4.12. High-performance Liquid Chromatography (HPLC) for Quantification of insulin

The concentration of insulin loaded onto PAA@rGO was determined by an HPLC system (Shimadzu, Tokyo, Japan) equipped with a 5 µm C18 AQ Uptisphere X ® , 250 mm × 4.6 mm column (Interchim, Montluçon, France) heated to 40 °C. The mobile phase consisted of a mixture of eluent A (formic acid 0.1% in water) and eluent B (formic acid 0.1 % in acetonitrile) at a flow rate of 1 mL/min. The samples were injected at a volume of 40 µL and the detection was recorded at a wavelength of 215 nm.

AUTHOR INFORMATION

Corresponding Author

*Email: sabine.szunerits@univ-lille.fr, Tel: +33 (0)3 62 53 17 25

ORCID

Amitav Sanyal: 0000-0001-5122-8329

Sabine Szunerits: 0000-0002-1567-4943

Rabah Boukherroub: 0000-0002-9795-9888

Bilal Delim: 0000-0003-1642-3481

Thomas Hubert: 0000-0002-5757-6436

Cristina Prieto: 0000-0002-0925-896X

Author Contributions: The manuscript was written through contributions of all authors.

Conflict of Interest. The authors declare no competing financial interest.

ACKNOWLEDGMENTS

The Centre National de la Recherche Scientifique (CNRS), the University of Lille, the Hauts-de-France region, and the CPER “Photonics for Society” are acknowledged for financial support. AV thanks the i-SITE foundation of the University of Lille for a PhD fellowship. This

project has received funding from the European Union's Horizon 2020 Research and Innovation Staff Exchange (RISE) Marie Skłodowska-Curie Actions under grant agreement No 690836. We acknowledge the help and involvement of the Dhure (Département Hospitalo-Universitaire de Recherche Expérimentale) platform in work related to the mini-pig.

References:

1. Huang, C.; Soenen, S. J.; Rejman, J.; Licas, B.; Braeckmans, K.; Demeester, J.; De Smedt, S. C., Stimuli-Responsive Electrospun Fibers And Their Applications. *Chem. Soc. Rev.* **2011,** *40*, 2417-2434.
2. Celebioglu, A.; Uyar, T., Hydrocortisone/Cyclodextrin Complex Electrospun Nanofibers for a Fast-Dissolving Oral Drug Delivery System. *RSC Med. Chem.* **2020,** *11*, 245-258.
3. Topuz, F.; Uyar, T., Electrospinning of Cylodextrin Functinal Nanobibers For Drug Delivery Applications. *Pharmaceutics* **2019,** *11*, 6.
4. Xue, J.; Wu, T.; Dai, Y.; Xia, Y., Electrospinning and Electropsun Nanofibers: Methods, Materials, And Applications. *Chem. Rev.* **2019,** *119*, 5298-5415.
5. Li, L.; Hsieh, Y.-L., Ultra-Fine Polyelectrolyte Fibers From Electrospinning Of Poly(Acrylic Acid). *Polymer* **2005,** *46*, 5133-5139.
6. Ning, Y.; Shen, W.; Ao, F., Application Of Blocking And Immobilization Of Electrospun Fiber In The Biomedical Field. *RSC Adv.* **2020,** *10*, 37246-37265.
7. Cao, S.; Hu, B.; Liu, H., *Polym. Int.* **2009,** *58*, 545.
8. Wallace, L. A.; Gwynne, L.; Jenkins, T., Challenges and Opportunities of pHIn Chronic Wounds *Therap. Deliv.* **2019,** *10*, 719-735.
9. Sofi, H. S.; A., A.-H.; Ivanovski, S.; Zhang, Y. S.; Sheikh, F., Electrospun Nanofibers For The Delivery Of Active Drugs Through Nasal, Oral And Vaginal Mucosa: Current Status and Future Perspectives. *Mater. Sci. Eng. C* **2020,** *111*, 110756.
10. Zhang, H.; Zhang, J.; Streisand, J. B., Oral Mucosal Drug Deliveryclinical Pharmacokinetics And Therapeutic. *Clin. Pharmacokinet.* **2002,** *41*, 661-680.
11. Shaikh, R.; Singh, T. R. R.; Garland, M. J.; Woolfson, A. D.; Donnelly, R. F., Mucoadhesive Drug Delivery Systems. *J. Pharm. Bioallied. Sci.* **2011,** *3*, 89–100.
12. Patel, V. F.; Fang, L.; Brown, M. B., Advances in Oral Transmucosal Drug Delivery. *J. Control. Release* **2020,** *153*, 106-116.
13. Illangakoon, U. E.; Gill, H.; Sherman, G. C.; Parhizkar, M.; S., M.; Chatterton, N. P.; Williams, G. R., Fast Dissolving Paracetamol/Caffeine Nanofibers Prepared By Electrosphinning. *Int. J. Pharm.* **2014,** *477*, 369-379.
14. Fonseca, D. F. S.; Costa, P. C.; Almeida, I. F.; Dias-Pereira, P.; Correia-Sa, I.; Bastos, V.; Oliveira, H.; Duarte-Araujo, M.; Morato, M.; Vilel, C.; Silvestr, A. J. D.; Freire, C. S. R., Pullulan Microneedle Pathces For The Efficient *Carbohydr. Polym.* **2020,** *241*, 116314.
15. Vaidyaa, A.; Mitragotri, S., Ionic Liquid-Mediated Delivery Of Insulin To Buccal Mucosa. *J. Control. Release* **2020,** *327*, 26.
16. Wright, A. K.; Kontopantelis, E.; Emsley, R.; Buchan, I.; Sattar, N.; Rutter, M. K.; Ashcroft, D. M., Life Expectancy And Cause-Specific Mortality In Type 2 Diabetes: A Population-Based Cohort Study Quantifying Relationships In Ethnic Subgroups. *Diabetes Care* **2017,** *40*, 338–345.
17. Pagneux, Q.; Ye, R.; Li, C.; Barras, A.; Hennuyer, N.; Staels, B.; Caina, D.; Avila Osses, J. I.; Abderrahmani, A.; Plaisance, V.; Pawlowski, V.; Boukherroub, R.; Melinte, S.;

Szunerits, S., Electrothermal Patches Driving the Transdermal Delivery of Insulin. *Nanoscale Horizon* **2020,** *5*, 663-670
18. Teodorescu, F.; Oz , Y.; Quéniat, G.; Abderrahmani, A.; Foulon, C.; Lecoeur, M.; Sanyal, R.; Sanyal, A.; Boukherroub, R.; Szunerits, S., Photothermally Triggered On-Demand Insulin Release from Reduced Graphene Oxide Modified Hydrogels. *J. Control. Release* **2017,** *246*, 164-173.
19. Thirion-Delalande, C.; Gervais, F.; Fisch, C.; Cuiné, J.; Baron-Bodo, V.; Moingeon, P.; Mascarell, L., Comparative Analysis of the Oral Mucosae From Rodents and Non-Rodents: Application To The Nonclinical Evaluation Of Sublingual Immunotherapy Products. *PLOS One* **2017,** *12*, E0183398.
20. Pinto, S.; Pintado, M. E.; Sarmento, B., In Vivo,Ex Vivo And In Vitro Assessment Of Buccal Permeation Of Drugs From Delivery Systems, . *Expert Opin. Drug Deliv.* **2020,** *17*, 33-48.
21. Pillai, O.; Panchagnula, R., Transdermal Delivery Of Insulin From Poloxamer Gel: Ex Vivo And In Vivo Skin Permeation Studies In Rat Using Iontophoresis And Chemical Enhancers. *J. Control. Release* **2003,** *89*, 127.
22. Altinbasak, I.; Jijie, R.; Barras, A.; Golba, B.; Sanyal, R.; Bouckaert, J.; Drider, D.; Bilyy, R.; Dumych, T.; Paryzhak, S.; Vovk, V.; Boukherroub, R.; Sanyal, A.; Szunerits, S., Reduced Graphene Oxide Embedded Polymeric Nanofiber Mats: An 'On-Demand' Photothermally-Triggered Antibiotic Release Platform *ACS Appl. Mater. Interfaces* **2018,** *10*, 41098-41106.
23. Franz-Montan, M.; Serpe, L.; Martinelli, C. C.; Da Silva, C. B.; Dos Santos, C. P.; Novaes, P. D.; Volpato, M. C.; De Paula, E.; Lopez, R. F. V.; Gropp, F. C., Evaluation Of Different Pig Oral Mucosa Sites As Permeability Barrier Models For Drug Permeation Studies. *Eur. J. Pharm. Sci.* **2016,** *81*, 52-59.